Applied Energy 383 (2025) 125374

Contents lists available at ScienceDirect

Applied Energy

journal homepage: www.elsevier.com/locate/apenergy

# Surrogate-assisted coordinated design optimization of building and microclimate considering their mutual impacts

Zeming Zhao [a], Hangxin Li [a,b,**], Shengwei Wang [a,c,*]

[a] Department of Building Environment and Energy Engineering, The Hong Kong Polytechnic University, Hong Kong, SAR, China
[b] Shenzhen Research Institute, The Hong Kong Polytechnic University, Shenzhen, China
[c] Research Institute for Smart Energy, The Hong Kong Polytechnic University, Hong Kong, SAR, China

## HIGHLIGHTS

- A coordinated design optimization method is proposed for a building and its microclimate.
- Mutual impacts between building design and local microclimate are considered.
- Pareto optimal solutions balance building energy efficiency and pedestrian thermal comfort.
- Energy consumption reduced by up to 63.34 %; thermal discomfort decreased by 1.88 K.
- 99.98 % reduction in computation time for surrogate-assisted design optimization over conventional simulation methods.

## ARTICLE INFO

*Keywords:*
Building design
Microclimate
Design optimization
Multi-objective optimization
Energy performance

## ABSTRACT

Building energy performance and pedestrian thermal comfort are strongly related and crucial in urban development. However, the mutual impacts of building design and local microclimate are often not quantitatively considered in design optimization due to their complex quantification. This study proposes a coordinated design optimization method that enables simultaneous optimization of both a building and its microclimate within a practically affordable time frame through an effective quantification method. SVR-based local air temperature and LightGBM-based local wind velocity surrogate models, along with automated building simulations, are integrated with the optimizer to enhance efficiency and generalizability. A total of eleven essential building design variables are optimized to minimize both total building energy consumption and pedestrian thermal discomfort. Global optimal solutions (i.e., Pareto front) identified by NSGA-II are evaluated using the entropy-TOPSIS method to determine the best solution. The proposed method is validated through a case study of a mixed-use building in Hong Kong. Results indicate that using the surrogate-assisted coordinated optimal design method can reduce the total building energy consumption by up to 63.34 % and pedestrian thermal discomfort degree by up to 1.88 K in subtropical regions. Additionally, computation time for design optimization is reduced by 99.98 % (i.e., from 42,684.44 to 8.89 h) compared to conventional simulation methods. This study fills a critical gap in the simultaneous design optimization to enhance building energy performance while balancing local microclimate impacts efficiently.

## 1. Introduction

Buildings are responsible for 30 % of the total global energy consumption and a third of carbon emissions in the worldwide, and they have huge potential to achieve carbon neutrality goals and combat global climate change [1,2]. The energy consumption of buildings is greatly influenced by their design, operation and the local microclimate surrounding them [3–7]. Conversely, buildings are also a primary factor influencing the local microclimate, particularly in high-density cities [8–12]. For instance, in Rome, a local air temperature rise of 2.8 °C could result in an increase of up to 74 % in building cooling load [12], while in Reading, UK, different building designs could cause the local air temperature rise of 0.27 to 0.73 K [13]. Therefore, it is essential to

* Corresponding author at: Research Institute for Smart Energy, The Hong Kong Polytechnic University, Hong Kong, SAR, China.
** Corresponding author at: Shenzhen Research Institute, The Hong Kong Polytechnic University, Shenzhen, China.
*E-mail addresses:* hangxin.li@polyu.edu.hk (H. Li), beswwang@polyu.edu.hk (S. Wang).

https://doi.org/10.1016/j.apenergy.2025.125374
Received 16 October 2024; Received in revised form 22 December 2024; Accepted 13 January 2025
Available online 22 January 2025

**Nomenclature**

| | |
|---|---|
| ACO | Ant Colony Optimization |
| CFD | Computational Fluid Dynamics |
| $d$ | Width of building (m) |
| $D_{discom}$ | Pedestrian thermal discomfort degree (°C) |
| $E_{tot}$ | Total building energy consumption (kWh/m$^2$) |
| $E_{LE}$ | Lighting electricity consumption (kWh/m$^2$) |
| $E_{EE}$ | Electricity consumption (kWh/m$^2$) |
| $E_{CE}$ | Cooling consumption (kWh/m$^2$) |
| GA | Genetic Algorithm |
| GIS | Geographic Information System |
| HypE | Hypervolume Estimation |
| LightGBM | Light Gradient Boosting Machine |
| MAE | Mean absolute error |
| NSGA-II | Non-dominated Sorting Genetic Algorithms |
| PET | Physiologically Equivalent Temperature (°C) |
| $PET_n$ | Neutral physiological equivalent temperature (°C) |
| $PET_{ave}$ | Average $PET$ (°C) |
| $PET_{male}$ | $PET$ of male (°C) |
| $PET_{female}$ | $PET$ of female (°C) |
| PSO | Particle Swarm Optimization |
| $Q_{CL}$ | Cooling demand of building (kWh/m$^2$) |
| RANS | Reynolds-Averaged Navier-Stokes |
| RSM | Response Surface Method |
| SA | Simulated Annealing |
| $SCOP_s$ | Overall coefficient of performance of air-conditioning system |
| SHGC | Solar Heat Gain Coefficient |
| SVR | Support vector regression |
| 3D | Three-dimensional |
| TOPSIS | Technique for order preference by similarity to ideal solution |
| UTCI | Universal Thermal Climate Index |

account for the mutual impacts between buildings and local microclimate in design optimization of buildings to enhance both building energy performance and outdoor thermal comfort.

In previous studies, the design optimization of buildings mainly focused on the design of building envelope and/or energy systems [14–30]. The design variables of building envelope usually concern the building layout and shape (e.g., orientation, footprint, aspect ratio, number of storeys, and window-to-wall ratio), thermal characteristics of building envelope (e.g., U-value, thermal absorptance, and solar absorptance), construction quality (e.g., air-tightness of façade, and linear coefficient of thermal bridges), and energy efficient strategy such as shading strategies (e.g., overhang projection ratio, overhang depth and overhang installation angle). The design variables of energy systems mainly include the number and capacity of system components (e.g., chiller plant, power generator, and energy storage). The design variables are generally optimized under typical meteorological weather condition to minimize building energy demand, life cycle cost or environmental impact e.g., carbon emissions and pollutant emissions), while maximizing the renewable power generation, indoor thermal comfort or visual comfort. Optimization methods such as genetic algorithm (GA), ant colony optimization algorithm (ACO), particle swarm optimization algorithm (PSO), response surface method (RSM), firefly algorithm, Manta-Ray foraging optimization algorithm and hypervolume estimation algorithm (HypE) are widely adopted. For instance, Li et al. made the coordinated optimal design of building envelope and energy systems using GA, which can efficiently save 4 % of total cost comparing with the uncoordinated design and reduce the accumulated unmet cooling loads by over 22 % [14]. Bui et al. used a modified firefly algorithm to optimize the design of an adaptive façade system in building, resulting in a reduction of 14.2–29.0 % in building energy consumption compared to static façades [29]. However, the mutual impacts between building design and local microclimate are not taken into consideration in the process of building design optimization [14–30].

With growing interest in urban microclimate in recent years, a few studies have attempted to address the environmental performance optimization through building design to enhance the wind flow and outdoor thermal comfort [31–40]. However, these studies normally focus on the optimal design of urban or district areas only [31,33,35–38,40]. Two studies investigated the impacts of buildings with a lift-up design [34,39]. Another study focused on the impacts of an individual building [32]. The variables to be optimized usually concern both the district morphology (e.g., building coverage ratio, plan area density, and building geometry configuration) and the building morphology (e.g., building width, depth, height, and orientation). Indexes such as the wind velocity ratio, the wind velocity Gini index, the Universal Thermal Climate Index (UTCI), and the Physiologically Equivalent Temperature (PET) are adopted to evaluate the wind flow and thermal comfort. The optimization methods include GA, Simulated Annealing (SA), the sequential quadratic programming method, and PSO. As the quantification of the impacts on the microclimate using high-resolution CFD simulations usually requires high computing cost, surrogate models based on machine learning algorithms are adopted to facilitate the design optimization, improving the computational efficiency, which is summarized in Table 1 [31–35,37–40]. Huang et al. combined a GAN-based surrogate model with the NSGA-II algorithm to achieve real-time optimization of urban morphology to increase urban block ventilation and reduce thermal discomfort, which has a time advantage over simulation when the number of optimized samples exceeds 174 [33]. Weerasuriya et al. utilized an ANN-based surrogate model to assist the lift-up design optimization of the main structure and center core to achieve the pedestrian wind comfort and thermal comfort of the areas surrounding the lift-up building [34]. Wu et al. focused on the design optimization of individual building morphology in the district to improve the pedestrian wind comfort, where the four building morphology variables (i.e. building width; depth; height and orientation) are optimized by the NSGA-II algorithm, assisted with Gaussian process regression surrogate model [32].

Based on the above review, the following gaps can be summarized regarding building design optimization for enhanced building energy performance and outdoor thermal environment.

- *The mutual impacts between building design and local microclimate (*i.e., *the impact of building design on the local microclimate and the impact of local microclimate on building performance) are usually ignored in building design optimization due to the complexity of their quantification, leading to significant bias of performance estimation, particularly for cases in high-density cities* [41]. In fact, current building design optimization is, indeed, of energy performance-driven [14–30]. But the building energy performance is usually evaluated under the typical meteorological weather condition of a city without considering the local microclimate.
- *Only very few studies have focused on the impacts of individual building design on local microclimate optimization* [32]. *However, some major influential building parameters, such as building envelope thermal characteristics, are not considered in the microclimate optimization.* Current studies mainly focus on the urban/district design optimization [31,33,35–38,40]. Indeed, the optimization of individual buildings is significant for the microclimate in high-density urban districts, and the development or renewal of buildings in existing districts is a common practice there.

**Table 1**
Representative studies on design optimization of local microclimate based on data-driven methods.

| Reference | Variables | Optimization objectives | Performance indicators | Optimization methods | Optimization scale | Application of surrogate model |
|---|---|---|---|---|---|---|
| [31] | Building width; building depth; floors number of high-rise building, mid-rise building and low-rise building | Maximize economic benefits; maximize outdoor wind comfort | Wind velocity ratio; wind velocity Gini index; gross profit | NSGA-II | District | Gradient boosted regression trees regression |
| [32] | Building width; building depth; building height; building orientation | Maximize summer and winter outdoor wind comfort | Positions meeting wind comfort level | NSGA-II | Target building | Gaussian process regression |
| [33] | Building coverage ratio; floor area ratio; average building height; standard deviation of building height; building shape factor; frontal area ratio | Maximize urban block ventilation; minimize heat and discomfort | Pedestrian level wind; radiation; UTCI | NSGA-II | District | Generative adversarial network (GAN) |
| [34] | Height and width of main structure; height, width, depth of central core; orientation of building | Maximize pedestrian wind comfort and thermal comfort | Percentage area of wind comfort; percentage area of thermal comfort | NSGA-II | Lift-up area of building | Artificial neural network (ANN) |
| [35] | Aspect ratio; ratio of long side to short side; horizontal rotation angle of building; corner cutting dimensions at corners of building | Minimize wind forces; minimize local strong winds around buildings; maximize heights of buildings in development area | Building height; along-wind force coefficient; wind velocity | GA; SA; sequential quadratic programming method | District | Convolutional neural network |
| [36] | Angle of central street segment, bridge location, building volumes. | Maximize outdoor wind comfort and thermal comfort | Minimize squared difference from target temperature, maximize comfortable area and minimize dangerous areas, maximize visitor potential, minimize average travel time | GA | City | – |
| [37] | Buildings heights configuration; plan area densities | Improve pedestrian-level wind conditions; minimize low-wind-speed regions; maximize outdoor urban ventilation; maximize outdoor wind comfort | Aerodynamic index of urban area | GA; PSO | District | – |
| [38] | Building densities; building plot ratios; building height; number of buildings in the plot; number of buildings in the columns; building spacing | Maximize outdoor wind comfort and thermal comfort | Sunshine hours; wind speed; solar radiation heat gain | GA | District | Multiple regression |
| [39] | Face-to-face gaps between buildings; height of upper building; height of lift-up core, width of lift-up core | Maximize pedestrian level wind comfort and thermal comfort | Area weighted mean wind velocity ratio; area weighted PET | NSGA-II | Lift-up area of building | Linear (first-order) and quadratic (second-order) regression |
| [40] | Buildings' layout in the block | Maximize indoor visual comfort and outdoor thermal comfort | Daylight factor; sky view ratio; window sunlight hours; site sunlight hours; UTCI | NSGA-II | District | ANN |

- *In the limited studies on local microclimate optimization, the impact on local air temperature is always ignored due to the complexity and high computational cost* [32], *which is also a primary factor affecting building performance and outdoor thermal comfort*. Only the wind environment is usually considered in local microclimate optimization.

In this study, a coordinated design optimization method is proposed, allowing the design optimization of a building and its microclimate to be achieved within a practically affordable time by adopting an effective quantification method. The multi-objective optimization aims to minimize both total building energy consumption and pedestrian thermal discomfort. Local microclimate surrogate models (i.e., SVR-based local air temperature model and LightGBM-based local wind velocity model) and automated building simulation are integrated with the optimizer to enhance the optimization efficiency and generalizability. Eleven essential building design variables can therefore be optimized with affordable computation efforts. The Pareto optimal solutions identified by NSGA-II are further evaluated using the entropy-TOPSIS method to determine the best solution. The proposed method is tested and validated by implementing it in a mixed-use development case in subtropical regions. This study efficiently addresses the need for simultaneous design optimization for enhancing building energy performance and mitigating adverse impacts on the local microclimate during the building envelope design stage.

Overall, the structure of the paper is organized as follows. Chapter 1 introduces the background and current state of research on building and microclimate optimization. Chapter 2 serves as the core of the paper, elaborating on the generic methodologies of coordinated design optimization, including the optimization procedure, problem formulation, objectives, building design variables to be optimized, and the necessity of coordinated design optimization, followed by the method for solution evaluation. Chapter 3 presents the validation case and the relevant constraints of the optimization design. Chapter 4 introduces the development of automated building performance simulation models and local microclimate surrogate models, which are computational tools to facilitate optimization. Chapter 5 presents the results and analysis of optimization case study. Chapter 6 draws up the conclusions and future works.

## 2. Methodologies of coordinated design optimization of building and its local microclimate

Several building design variables, such as building aspect ratio and building orientation, considered in this study, have opposite effects on the two performance objectives, i.e., building energy performance and local environmental performance, as elaborated in Section 2.5.

Therefore, the proposed coordinated design optimization considering the mutual impacts of a building and its microclimate is essential. The mutual impacts refer to the interactions between a building and its local microclimate. Building design affects the local microclimate (i.e. local air temperature and local wind velocity) surrounding the building; meanwhile, the microclimate affects the building energy performance. The impacts of building design on local microclimate are taken into consideration when evaluating the environmental performance optimization objective. Additionally, the impacts of local microclimate on building energy performance are taken into consideration in evaluating the energy performance optimization objective.

### 2.1. Overall procedure and major steps

The multi-objective optimization is adopted for the coordinated optimal design of a building and its local microclimate to effectively identify the global optimal design solutions, considering their mutual impacts. The detailed procedure of the coordinated design optimization is illustrated in Fig. 1.

The coordinated design optimization involves energy performance-driven design and environmental performance-driven design. The building design variables affecting building energy performance and local microclimate are optimized. The ranges of the variables are preset for the optimizer to generate building design options. Multi-objective optimization is conducted using the non-dominated evolutionary algorithm NSGA-II [42], which minimizes the optimization objectives of both energy performance-driven design and environmental performance-driven design, subject to the satisfaction of the design constraints.

The optimization objective of energy performance-driven design is calculated using automated building performance simulation in the software Energyplus, which is integrated with the optimizer through the Eppy toolkit in Python to ensure the generalizability, fidelity, and automation. The optimization objective of environmental performance-driven design is calculated using the local microclimate surrogate models with high accuracy and high efficiency, including an SVR-based surrogate model of local air temperature and a LightGBM-based surrogate model of local wind velocity. These surrogate models are developed based on the typical scenario of a high-density urban district which can ensure the model generalizability. The results of numerous 3D high-resolution microclimate simulations based on CFD simulation and advanced GIS spatial analysis techniques are used for the surrogate model development. The prediction results of local microclimate under different building design options are provided not only for the calculation of environmental performance-driven design objective concerning the pedestrian thermal comfort, but also for the automated building energy performance simulation, in order to consider the mutual impacts between building design and local microclimate.

Based on the energy and environmental performance evaluation of the building design options, the optimizer identifies the Pareto front including a few global optimal solutions of simultaneous building and local microclimate optimization. Finally, the Pareto optimal solutions are evaluated and the best design solution is recommended using the entropy-TOPSIS method.

In this study, two major efforts have been made to enhance the efficiency, generalizability, and automation of the optimization model. Firstly, the automated building performance simulation, using the software EnergyPlus, is integrated with the optimization technique through the Eppy toolkit in Python. Once design optimization is required in a new design scenario, the building performance simulation will proceed automatically with only the need to modify the ranges of building design variables and settings of parameters in Python. Secondly, the surrogate models of local microclimate are also integrated with the optimization solver, which predicts the local microclimate instantaneously given the ranges of design variables for a new design scenario.

### 2.2. Formulations of the optimization problem

The coordinated design optimization problem of a building and its local microclimate is formulated as Eq. (1). Where, $F$ is the design optimization objective. $F_{ene}$ is evaluates energy performance, as illustrated in Section 2.3.1. $F_{env}$ evaluates environmental performance, as illustrated in Section 2.3.2. $X$ refers to the eleven building design

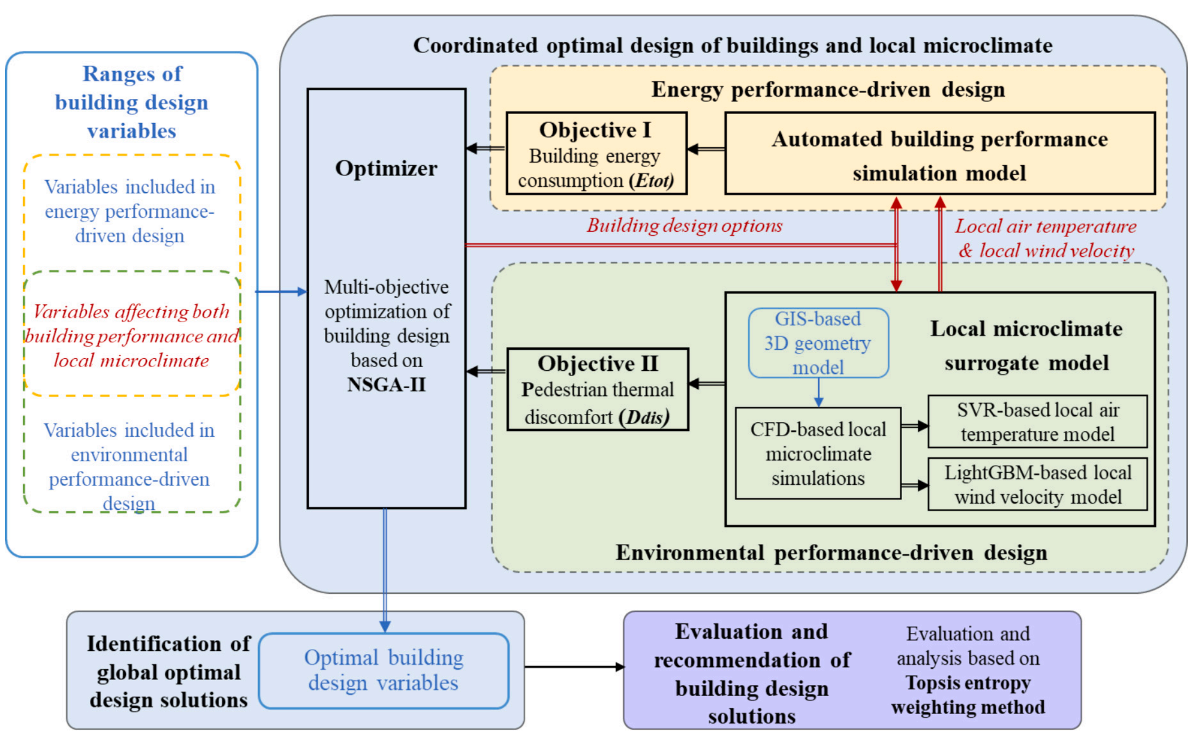


**Fig. 1.** Outline of the coordinated design optimization of building and its local microclimate.

variables, which will be illustrate in Section 2.4. $X_{min}$ is the lower bound of the search range for the design variables. $X_{max}$ is the upper bound, as shown in Table 2. The building design variables are optimized within their search ranges, subject to the design constraint $C$ as shown in Eq. (2), which will be illustrated in Section 3.

$$Minimize: F = (F_{ene}, F_{env}) \tag{1}$$

$$subject\ to: X_{min} \leq X \leq X_{max}$$

$$C(X) \leq 0 \tag{2}$$

## 2.3. Optimization objectives

In this study, two design objectives are adopted in the coordinated design optimization. One evaluates the energy performance of the building, and the other evaluates the local environmental performance surrounding the building.

### 2.3.1. Optimization objective evaluating energy performance

The energy performance objective ($F_{ene}$) is formulated as shown in Eqs. (3) [43], which evaluates the building energy consumption affected by the local microclimate. The total building energy consumption includes the total electricity consumption for cooling, lighting and other equipment on a typical design day. The total building energy consumption on a typical design day is chosen as the optimization objective because it significantly reduces computation time during the iterative optimization process. This approach allows for a quick evaluation of energy consumption across different building envelope design schemes while achieving similar optimization results compared to the total building energy consumption for the entire cooling season. On a typical summer design day, the total building energy consumption reflects the maximum daily energy use under unfavorable conditions. A lower energy consumption during this typical condition indicates effective building envelope design.

The building design variables are optimized to minimize this objective to achieve a higher energy efficiency for the building designed. This objective is quantified by the automated building energy performance simulation under the most unfavorable weather condition, i.e., the typical summer design day under clear sky conditions, which accounts for the local microclimate effect. The typical summer design day under clear sky conditions is utilized to assess the building energy consumption under extreme climate conditions. Thus, the representative daily building energy consumption can be analyzed [44,45].

$$F_{ene} = E_{tot} = E_{CE} + E_{LE} + E_{EE} = Q_{CL}/\mathrm{SCOP}_s + E_{LE} + E_{EE} \tag{3}$$

where, $E_{tot}$ is total building energy consumption (kWh/m$^2$). $E_{CE}$ is the electricity consumption for cooling (kWh/m$^2$), calculated based on the cooling demand ($Q_{CL}$) of the building (kWh/m$^2$) and the overall coefficient of performance of the air-conditioning system ($SCOP_s$). In this study, $SCOP_s$ is set to 4. $E_{LE}$ is the lighting electricity consumption (kWh/m$^2$). $E_{EE}$ is the electricity consumption (kWh/m$^2$) of other electric equipment.

**Table 2**
Design variables to be optimized by the coordinated optimal design.

| Design variable | Abbreviation | Search range | Unit |
|---|---|---|---|
| Overhang tilt angle | OTA | [0,180] | ° |
| Window SHGC | WSHGC | (0,0.48] | |
| Window to wall ratio | WWR | [0.1,0.4] | – |
| Wall solar absorptance | WSA | [0.1,0.9] | – |
| Skylight SHGC | SSHGC | [0.1,0.3] | |
| Skylight to roof ratio | SRR | (0,0.9] | – |
| Building height | BH | [6200] | m |
| Building aspect ratio | BAR | [1,9] | – |
| Overall heat transfer coefficient of building envelope | OHTC | [1.1,14.0] | W/(m$^2$•K) |
| Building orientation | BO | [0,360) | ° |
| Emissivity of wall | EW | (0,1) | – |

### 2.3.2. Optimization objective evaluating environmental performance

The environmental performance objective ($F_{env}$) is adopted to evaluate the pedestrian thermal discomfort under the local microclimate, which is affected by the building design. It is formulated based on PET, as shown in Eqs. (4–5). PET is a widely used outdoor thermal comfort index that assesses the impact of environmental temperature on human thermal comfort. It is defined as the air temperature at which the human body's heat balance is maintained, with core and skin temperatures equal to those under the assessed conditions [50]. The building design variables are optimized to minimize this objective to improve the outdoor thermal comfort surrounding the building. In this study, the term "pedestrian-level" refers to the position that is 3.0 m away from the building and at a height of 1.5 m. This objective is quantified under the most unfavorable weather condition, i.e., during the hottest hour in the typical summer design day under clear sky conditions with the prevailing wind condition. The hottest hour is utilized to assess the pedestrian thermal discomfort under extreme climate conditions, ensuring that maximum discomfort is minimized and leading to improved outdoor thermal comfort throughout the typical design day. This approach allows for effective optimization of pedestrian thermal discomfort while significantly reducing computational costs [8,9,46–49].

$$F_{env} = D_{dis} = |PET_{ave} - PET_n| \tag{4}$$

$$PET_{ave} = \left(PET_{male} + PET_{female}\right)/2 \tag{5}$$

where, $D_{dis}$ is the pedestrian thermal discomfort degree (°C). A higher absolute value indicates a higher degree of thermal discomfort. $PET_n$ is the neutral physiological equivalent temperature, which is set to 28 °C in Hong Kong [50]. $PET_{ave}$ is the average $PET$ of male ($PET_{male}$) and female ($PET_{female}$). The $PET_{male}$ and $PET_{female}$ are calculated by pythermalcomfort.models toolkit in Python utilizing the developed local microclimate surrogate models.

## 2.4. Building design variables concerned

A total of eleven building design variables affecting building energy performance and local microclimate are considered in the coordinated design optimization. They are the overhang tilt angle, window SHGC (Solar Heat Gain Coefficient), window to wall ratio, wall solar absorptance, skylight SHGC, skylight to roof ratio, building height, building aspect ratio, overall heat transfer coefficient of building envelope, building orientation and emissivity of wall. Overhang tilt angle refers to the angle at which an overhang (a roof extension) is tilted relative to the horizontal plane, which affects the shading performance. SHGC (solar heat gain coefficient) is the ratio of the amount of solar radiation heat entering through the window or transparent material to the total solar radiation heat reaching the surface of the window or transparent material. A higher SHGC indicates that the window allows more solar heat to enter the building. Skylight SHGC measures the solar radiation admitted through the skylight. Building aspect ratio is the ratio of the building's length to its width. Overall envelope heat transfer coefficient is the combination of heat transfer coefficient of wall and window, which is formulated as Eq. (6).

$$U_{overall} = U_{window} \bullet WWR + U_{wall} \bullet (1 - WWR) \tag{6}$$

where, $U_{overall}$ is overall envelope heat transfer coefficient (W/(m$^2$•K)). $U_{window}$ is overall envelope heat transfer coefficient of window (W/(m$^2$•K)). $WWR$ is window to wall ratio. $U_{wall}$ is overall envelope heat transfer coefficient of wall (W/(m$^2$•K)).

These design variables are selected based on the results of a systematic and comprehensive sensitivity analysis on the key building design parameters affecting building energy performance and local microclimate in subtropical regions [43,51]. It has been found that building height is negatively correlated with both building energy consumption and pedestrian thermal discomfort, primarily due to shading effects and ambient wind velocity [51]. Conversely, the heat transfer coefficient is positively correlated with building energy consumption and pedestrian thermal discomfort due to heat loss [51]. In summer, low emissivity of walls may result in higher pedestrian thermal discomfort [51]. Building aspect ratio and building orientation exert opposite effects on these two performance objectives, which will be elaborated in Section 2.5. The overhang tilt angle is critical for high-rise buildings across all climate zones. Furthermore, parameters such as window SHGC, window-to-wall ratio, wall solar absorptance, skylight SHGC, and skylight-to-roof ratio are highly sensitive factors affecting building energy consumption for both high-rise and low-rise buildings in subtropical regions [43]. These variables are optimized in their search ranges as listed in Table 2. The ranges are determined according to the requirements of building energy efficiency [52–54] and the settings in previous studies [3,10,43,55].

### 2.5. The need of coordinated design optimization

In this section, the need for coordinated design optimization of a building and its local microclimate is elaborated. Fig. 2 shows the relationship between the design variables and objectives of the energy performance-driven design and the environmental performance-driven design. The positive sign indicates a positive relationship between the design variable on the optimization objective, while the negative sign refers to the negative relationship. The impacts are investigated in a previous study by the authors [43,51]. It can be seen that there are four building variables affecting both building energy performance and local microclimate: building height, building aspect ratio, overall heat transfer coefficient of building envelope and building orientation. However, some of these design variables (i.e. building aspect ratio and building orientation) have opposite effects on the two optimization objectives (i.e. total building energy consumption and pedestrian thermal discomfort degree). The increase of building aspect ratio leads to higher building energy consumption but lower pedestrian thermal discomfort. Similarly, when the building orientation is increased, the

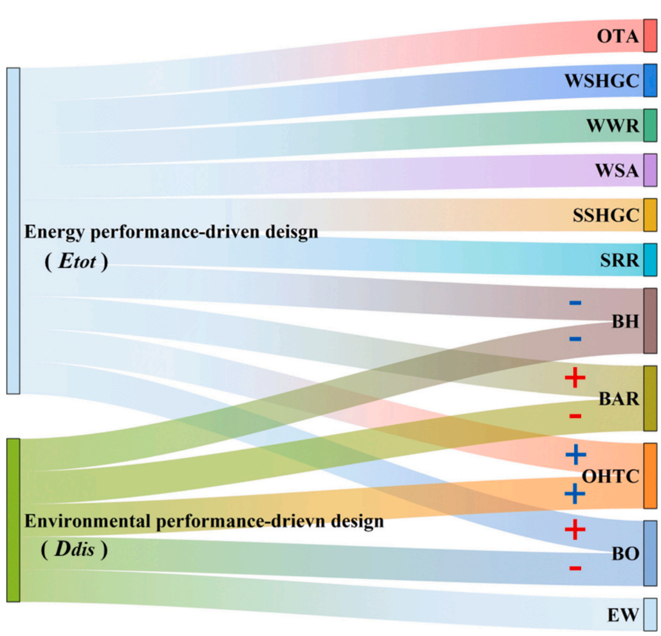


**Fig. 2.** The relationship between design variables and objectives of the energy performance-driven design and the environmental performance-driven design.

pedestrian thermal discomfort decreases but the building energy consumption increases. That means that a building design which has the lowest building energy consumption may not be conducive to the local microclimate. Therefore, it is necessary to coordinate the building and local microclimate design to make a balance between the improvements of building energy performance and local microclimate.

Although some design variables are key for the energy performance objective while others are key for the environmental performance objective, it is necessary to include all variables in the multi-objective optimization. Firstly, the impacts of design variables on the objective are complex and not monotonic; positive and negative relationships only hold to a certain extent. Larger or smaller values may not be always better. Second, the two optimization objectives mutually restrict each other, requiring a trade-off between the them. Besides the common variables, other variables that significantly impact on one objective also slightly impact on the other objective, the complex and subtle interactions between variables and objectives will also be considered in the trade-off.

### 2.6. Entropy-TOPSIS method for solution evaluation

In this study, the entropy-TOPSIS method is utilized for the evaluation of the Pareto optimal solutions obtained by the coordinated design optimization to select the best solution maximizing the overall benefits concerning building energy performance and pedestrian thermal comfort. The entropy-TOPSIS method mainly includes two stages. In the first stage, Shannon's entropy weight method is utilized to give weight to each design variable which is determined to be the evaluation criteria in this study. In the second stage, the TOPSIS technique is applied to rank the Pareto optimal solutions.

Shannon's entropy is a measure of the uncertainty in information representing the average intrinsic information transmitted for decision-making [56]. The smaller the information entropy, the greater the weight. Shannon's entropy weight method includes the process of normalization of the decision matrix, calculation of information entropy and calculation of weight for evaluation criteria. In order to make comparisons across the evaluation criteria, the data in the decision matrix with various criterion dimensions are normalized to a non-dimensional criterion. The decision matrix is normalized as $P = [p_{i,j}]$ $m \times n$, $i = 1,2, \ldots,m$; $j = 1,2, \ldots,n$. In this study, $p_{i,j}$ is the value of the building design variable in a design scheme after normalization. $m$ is determined as 14 which is the number of Pareto optimal solutions to be evaluated, $n$ is determined as 11 which is the number of evaluation criteria. The information entropy for each evaluation criteria is formulated as Eq. (7). The weight given to each evaluation criterion is formulated as Eq. (8). The weighted matrix is formulated as Eq. (9).

$$E_j = -(\ln m)^{-1}\sum_{i=1}^{m} p_{i,j}\ln p_{i,j} \tag{7}$$

$$w_j = (1 - E_j) \Bigg/ \left(n - \sum_{j=1}^{n} E_j\right) \tag{8}$$

$$p_{i,j}^{w} = w_j \bullet p_{i,j} \tag{9}$$

The technique for order preference by similarity to ideal solution (TOPSIS) used for ranking is one of the well-known methods in multi-criteria decision making. The best solution determined by TOPSIS has the shortest distance to the positive ideal solution while having the farthest distance to the negative ideal solution. The positive ideal solution can maximize the benefit criteria and minimize the cost criteria. On the contrary, the negative ideal solution can maximize the cost criteria and minimize the benefit criteria [57]. The positive ideal solution and negative ideal solution of each evaluation criterion can be determined using Eq. (10−11), respectively. The Euclidean Distance of each Pareto optimal solution to the positive ideal solution and the negative ideal solution is formulated as Eq. (12−13). The relative closeness of each

Pareto optimal solution to the ideal solution, which is used as a score for the comprehensive evaluation, is formulated as Eq. (14). The larger the value is, the closer the solution is to the positive idea solution, and the better the design performance of the solution will be.

$$p_j^+ = max\left(p_{i,j}^w\right), \mathrm{i} \in [1, \mathrm{m}] \tag{10}$$

$$p_j^- = min\left(p_{i,j}^w\right), \mathrm{i} \in [1, \mathrm{m}] \tag{11}$$

$$d_i^+ = \sqrt{\sum_{j=1}^{n}\left(p_{i,j}^w - p_j^+\right)^2}, \mathrm{i} \in [1, \mathrm{m}] \tag{12}$$

$$d_i^- = \sqrt{\sum_{j=1}^{n}\left(p_{i,j}^w - p_j^-\right)^2}, \mathrm{i} \in [1, \mathrm{m}] \tag{13}$$

$$C_i = d_i^- / \left(d_i^+ + d_i^-\right), \mathrm{i} \in [1, \mathrm{m}] \tag{14}$$

## 3. Description of the validation case and design constraints

The proposed coordinated optimal design method for a building and its local microclimate is validated in a typical scenario where a new mixed-use building is developed within an existing urban area, as shown in Fig. 3. Currently, the development or renewal of individual buildings in an existing district is a more common practice compared with the full development of entire districts in the high-density urban area, due to the limited available spaces. An example of the building geometry model is shown in Fig. 4. The building, functioning as a student dormitory, will be located in Kowloon, Hong Kong, which is an urban area characterized by high-density and high-rise developments in subtropical regions. The building operates 24 h a day, on every day.

Some constraints on the building geometry are considered in the coordinated design optimization, which is shown in Eqs. (15–16). The building volume for each building design option is fixed to provide the expected floor area for accommodating occupants, which is determined as 127,500 $m^3$ in this study. The width of the new building is constrained within a range from 15 m to 125 m, considering the minimum width requirements and the maximum available site area.

$$BH \bullet BAR \bullet d^2 = 127500 \tag{15}$$

$$15 \ll d \ll 125 \tag{16}$$

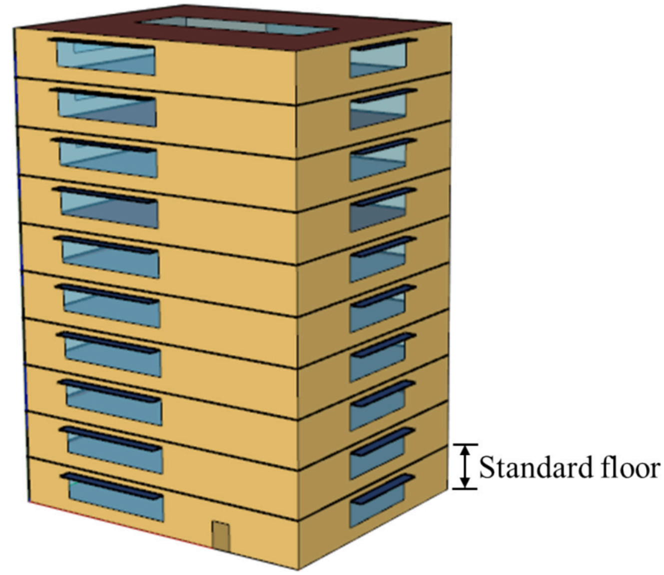


**Fig. 4.** An example of the building geometry model for coordinated optimal design.

where, *BH* is the building height (m). *BAR* is the building aspect ratio. *d* is the width of the new building (m).

## 4. Development of automated building performance simulation model and local microclimate surrogate models

### 4.1. Automated building performance simulation model

The building performance model is developed using the software EnergyPlus and integrated with the optimization technique through the Eppy toolkit in Python, allowing for real-time evaluation of building energy performance during the iteration process. The results of energy performance design objectives can be continuously and automatically fed back to the optimization model. The simulation can proceed automatically with only the modification of simulation model settings in Python, resulting in high automation for convenient implementation in new building design scenarios. The simulation process is efficient, taking approximately four seconds for a single simulation. Given the manageable computational time, there is no need to develop surrogate models

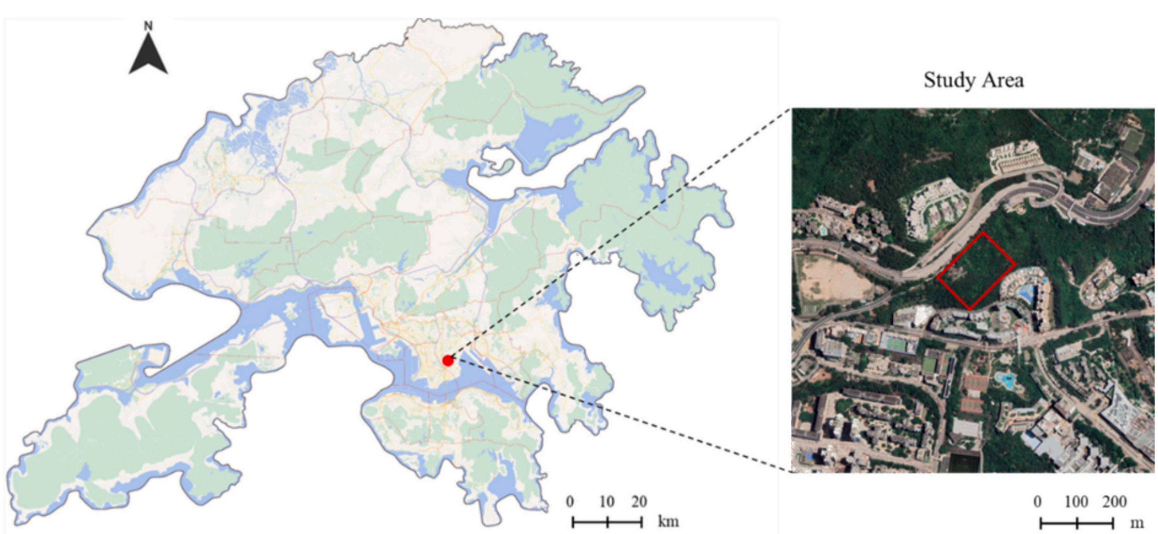


**Fig. 3.** Aerial view of the study area and the location of the new building.

for specific scenarios, thereby enhancing the fidelity and generalizability of the building performance simulation.

The mutual impacts between a building and its local microclimate are taken into consideration in the automated building performance simulation model. The weather data, incorporating local microclimate impacts, is used as the inputs for each building performance simulation. It is generated by adding the changes of the local microclimate, affected by the building design, to the original TMY (typical meteorological year) data on the typical summer design day. The local microclimate impacts refer to changes in local air temperature and wind velocity caused by different building designs. These impacts are predicted by the developed surrogate models of local air temperature and wind velocity to be introduced in Section 4.2.

An example of the building geometry model used in simulation is shown in Fig. 3. The logic of coordinated natural ventilation and air-conditioning controls adopted in the simulation is shown in Fig. 5. Natural ventilation and daylighting are utilized as much as possible in order to minimize energy consumption [43]. The ideal air system is utilized to simulate cooling demand, allowing for a rapid assessment of the energy performance of various building envelope design schemes during the optimization process. This simplified model assumes uniform output levels for HVAC equipment across all design schemes.

### 4.2. Local microclimate surrogate models

The fast and efficient surrogate models of local microclimate (i.e., SVR-based local air temperature surrogate model and LightGBM-based local wind velocity surrogate model) are utilized to predict the local microclimate impacts affected by different building designs. They are adopted in order to significantly reduce the computing time while maintaining the same order of accuracy as CFD simulations. Two single-output surrogate models are developed for predicting the local air temperature and wind velocity respectively, which are the major microclimate parameters affecting thermal comfort. These surrogate models utilize different machine learning algorithms because various machine learning methods are appropriate for different prediction purposes, and they demonstrate higher accuracy than multi-output

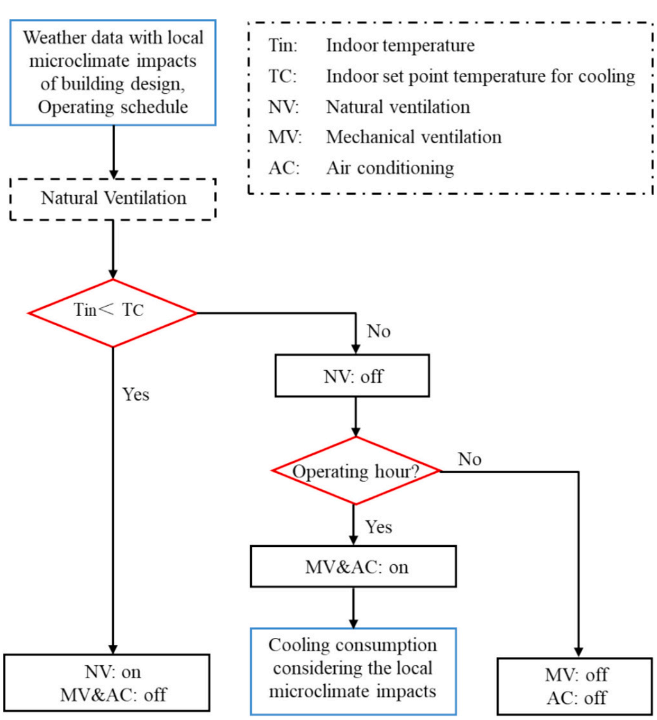


**Fig. 5.** Logic of coordinated natural ventilation and air-conditioning controls in simulation.

surrogate model in the test and validation [49,58,59].

The inputs of the surrogate models are five key building design variables affecting local microclimate, as shown in Fig. 2. To enhance the generalizability of the surrogate model, the relative changes in the local microclimate before and after the addition of a new building are set as the model outputs. The output of the SVR-based local air temperature surrogate model is the change in the local air temperature affected by the building design. The output of the LightGBM-based local wind velocity surrogate model is the change in the local wind velocity affected by the building design. Compared with existing models directly using the local microclimate parameters as the model outputs, the surrogate models developed in this study can significantly reduce the dependency on the climate conditions. Thus, they can be applied to predicting microclimate changes affected by individual buildings under different weather conditions. The position for evaluating the changes is at pedestrian level (i.e., 3.0 m away from the building and at a height of 1.5 m), which is the same as the position used for assessing pedestrian thermal discomfort in the coordinated design optimization.

The surrogate models of high computing efficiency and prediction accuracy have been developed in a previous study by the authors [49]. They are developed using the same scenario as the validation case for the coordinated design optimization shown in Fig. 3, which is applicable to the development of individual buildings in an existing district within a high-density urban area. 200 sets of high-resolution 3D microclimate simulation data corresponding to different building designs are used as the dataset for the model development. The high-resolution CFD simulation and advanced GIS spatial analysis techniques are used to provide microclimate data of high accuracy. 3D steady Reynolds-Averaged Navier-Stokes (RANS) is used for the CFD simulation model. The detailed settings of the computational domain, grid systems and boundary conditions can refer to previous studies by the authors [49,51]. The validation of the CFD model is conducted in order to ensure the fidelity of the CFD simulation results. The boundary conditions and parameter settings of the CFD model are validated by comparing the numerical modeling results with the wind tunnel test data of Case E wind tunnel experiment made by Architecture institute of Japan (AIJ) [60].

The 200 cases are generated using the Latin hypercube sampling method [61] to significantly reduce the sample size. LHS is utilized to reduce the sample size needed for developing an accurate surrogate model while ensuring good distribution and representativeness of the sample points in the design space [62]. Consequently, the entire design space can be explored efficiently with fewer samples, and the obtained data samples are representative and informative for economically constructing a surrogate model [63]. The sample size of 200 is determined by balancing the time-consuming data generation of CFD simulations and the adequacy of model training to obtain good prediction accuracy, which well meets the rules of optimum sample size for LHS [63–65]. The appropriateness of the sample size has been validated by estimating the accuracy of surrogate models utilizing 10-fold cross validation [49].

The surrogate models have been validated in terms of the prediction accuracy, the balance of model fit and complexity, and computational load [49]. The developed SVR-based local air temperature surrogate model has a high prediction accuracy (i.e., MAE of 0.194 °C, MSE of 0.065 °C, normalized RMSE of 0.187 and MAD of 0.120 °C) It demonstrates a good performance in balancing the model fit and complexity to mitigate the risk of overfitting, with an AIC (Akaike Information Criterion) of 50.055 and a BIC (Bayesian Information Criterion) of 56.029. The LightGBM-based local wind velocity surrogate model has an MAE of 0.352 m/s, MSE of 0.192 m/s, normalized RMSE of 0.212 and MAD of 0.335 m/s. It also performs well in balancing model fit and complexity to mitigate the risk of overfitting, with an AIC of 52.604 and a BIC of 58.578. The prediction time for both surrogate models is at the millisecond level for each prediction. The computations are performed on a PC with an i7–3770 CPU at 3.40 GHz and Windows 7 Enterprise 64-bit OS using the Scikit-learn machine learning library in Python 3.2.2 (64-

bit). The generalizability and automation of the models are enhanced by incorporating various design scenarios into model training and integrating the model with an optimization technique in Python [49].

## 5. Results and analysis of optimization case study

### 5.1. Optimal design results of building and its local microclimate

The purpose of the coordinated design optimization is to identify the global optimal building design solutions that minimize both total building energy consumption ($E_{tot}$) and the pedestrian thermal discomfort ($D_{dis}$), by considering the interactions between the building and its local microclimate. The NSGA-II algorithm is adopted in this study for the multi-objective optimization due to its good performance and fast convergence speed. It has the structure of an evolutionary algorithm, in which the non-dominated sorting approach and crowded comparison operator are utilized to rank and preserve the elitist solutions [32]. The initial population was set at 100 designs, and 80 iterations were conducted for the evolutionary search process to converge and obtain the final Pareto solutions. The convergence criteria for the optimization algorithm are set to $10^{-6}$.

The historical samples of building design and the identified Pareto optimal set in the coordinated design optimization are shown in Fig. 6. A total of ten global optimal solutions are identified as the Pareto front, each of which is not dominated by other solutions. The detailed optimization results are listed in Table 3. Notably, the design solution with the lowest energy consumption also results in the highest level of pedestrian thermal discomfort, reflecting the trade-off between energy performance and thermal comfort in the coordinated design optimization. If the priority of the building design is to improve building energy performance, the total building energy consumption on typical summer design day can be as low as 0.060 kWh/m$^2$ while the pedestrian thermal discomfort degree would be 8.580 °C. The building energy consumption under this scenario is reduced by up to 63.34 % (0.104 kWh/m$^2$) compared with historical samples. Conversely, as the pedestrian thermal comfort improves, the building energy consumption increases; thus, the design solution with the lowest pedestrian thermal discomfort results in the highest energy consumption. When the priority is to improve pedestrian thermal comfort, the pedestrian thermal discomfort degree can be as low as 7.785 °C, which is reduced by 9.3 % (i.e., 0.795 K) compared to the scenario where the priority is given to building energy performance, and is reduced by 19.41 % (i.e., 1.875 K) compared with historical samples. The building energy consumption on a typical summer design day under this scenario is 0.066 kWh/m$^2$, which is increased by 0.007 kWh/m$^2$ compared to the scenario where the priority is given to building energy performance. The trade-off occurs when certain building design variables have conflicting impacts on the two performance objectives: total building energy consumption and pedestrian thermal discomfort. This aligns with the results of the previous sensitivity analysis, which indicates that building aspect ratio and orientation are positively correlated with energy consumption (spearman correlation coefficient values of 0.3 and 0.1, respectively) and negatively correlated with pedestrian thermal discomfort (spearman correlation coefficient values of −0.1 for both) [51]. As shown in Table 3, when the building aspect ratio increases from 1.3 (in Scheme 1) to 1.8 (in Scheme 10), total building energy consumption rises from 0.060 to 0.066 kWh/m$^2$, while thermal discomfort decreases from 8.58 °C to 7.79 °C. A lower aspect ratio results in a more compact building geometry, reducing heat exchange between the interior and exterior, thereby lowering energy consumption. Conversely, a larger aspect ratio makes the building resemble a flat plate, which can promote ventilation around it, increasing wind velocity and lowering air temperature, thus mitigating pedestrian thermal discomfort in summer. Therefore, trade-offs are needed to balance building energy performance and pedestrian thermal comfort by optimizing variables such as building aspect ratio. The optimal range for building orientation is relatively narrow, only between 8.2° and 18.0° (with a search range of 0° to 360°). Its impact on total building energy consumption and pedestrian thermal discomfort is weaker and more complex. Different orientations are influenced by shading and natural ventilation in varying ways. When variables do not exhibit a monotonic relationship with the objectives, coordinated design optimization becomes essential to balance their effects and identify the optimal design solutions.

The search range, mean value, median value and distribution of the Pareto front of the building design variables are shown in Fig. 7. It can be observed that within a wide range of the variables to be optimized, the impact of variables on energy consumption and thermal discomfort is not monotonic. The Pareto front suggests that the optimal range for overhang tilt angle is 125–170°, window SHGC is 0.01–0.06, window to wall ratio is 0.2–0.3, wall solar absorptance is around 0.1, skylight SHGC is around 0.3, skylight to roof ratio is 0.01–0.05, building height is 180–191 m, building aspect ratio is 1.3–1.8, overall heat transfer coefficient of building envelope is 1.5–5.7 W/(m$^2$•K), building orientation is 8–18°, and emissivity of wall is 0.6–0.7 which can minimize the building energy consumption while mitigating the pedestrian thermal discomfort in the test case.

The optimization results of window SHGC, window to wall ratio, skylight SHGC and skylight to roof ratio can effectively meet the Chinese standards for near zero energy buildings and energy efficiency of buildings in subtropical regions [52–54]. Low-emissivity glass with a specialized coating can effectively reflect infrared radiation while allowing visible light to pass through, resulting in a low SHGC. Additionally, multi-layered glass structures can offer better insulation and have the potential to achieve such a low SHGC for windows or skylights. Within the permissible range, a larger overhang angle can more effectively block sunlight and reduce solar heat gain, thus reducing the energy consumption for cooling. A smaller wall solar absorptance can reduce the solar heat gain of the wall, consequently decreasing the cooling load of the building. Currently, high-reflectivity coatings in white or light colors are widely used to significantly reduce solar absorptance, achieving an absorptance of 0.1 or lower.

As for the four design variables involved in both energy performance-driven design and environmental driven-design, a larger building height and more compact building geometry (i.e., BAR of 1.3–1.8) are suggested in this optimization case, however, an optimal range of height (i.e., 180 to 191 m) is proposed rather than pursuing sheer magnitude. A high-rise building with a low aspect ratio has relatively few interface areas for conducting heat exchange with the outdoors, thus reducing the building energy demands [66,67]. Meanwhile, the effects of the vertical

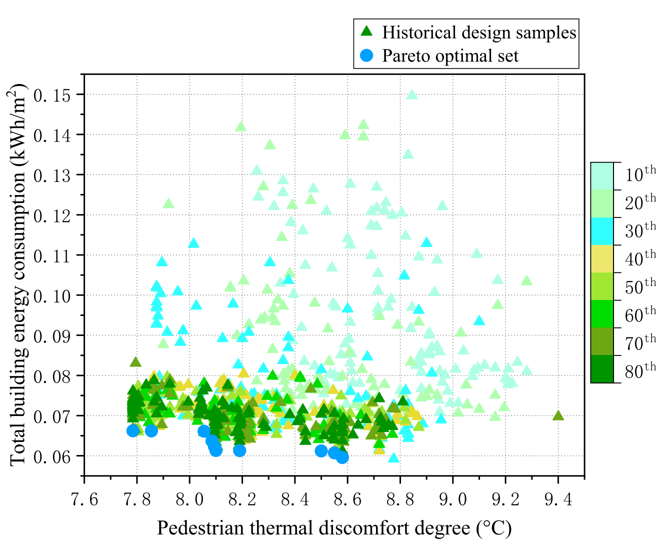


**Fig. 6.** Historical samples of building design (10th to 80th generation) and Pareto optimal set in the coordinated design optimization.

**Table 3**
Pareto optimal solutions of the coordinated design optimization of building and local microclimate.

| Scheme number | Building design variables | | | | | | | | | | | Optimization objectives | |
|---|---|---|---|---|---|---|---|---|---|---|---|---|---|
| | OTA (°) | WSHGC | WWR | WSA | SSHGC | SRR | BH (m) | BAR | OHTC (W/(m$^2$•K)) | BO (°) | EW | $E_{tot}$ (kWh/m$^2$) | $D_{dis}$ (°C) |
| 1 | 169.607 | 0.015 | 0.237 | 0.104 | 0.255 | 0.051 | 188.260 | 1.288 | 1.508 | 18.021 | 0.683 | 0.05959 | 8.580 |
| 2 | 125.856 | 0.015 | 0.257 | 0.107 | 0.256 | 0.052 | 186.339 | 1.298 | 1.510 | 11.664 | 0.682 | 0.06075 | 8.550 |
| 3 | 161.050 | 0.020 | 0.187 | 0.104 | 0.269 | 0.049 | 180.446 | 1.530 | 1.555 | 8.356 | 0.641 | 0.06123 | 8.500 |
| 4 | 146.566 | 0.007 | 0.233 | 0.108 | 0.251 | 0.007 | 187.638 | 1.328 | 1.578 | 10.028 | 0.629 | 0.06131 | 8.190 |
| 5 | 156.230 | 0.059 | 0.194 | 0.102 | 0.255 | 0.044 | 186.344 | 1.827 | 2.021 | 8.220 | 0.629 | 0.06133 | 8.100 |
| 6 | 144.303 | 0.014 | 0.188 | 0.127 | 0.256 | 0.053 | 186.343 | 1.848 | 1.597 | 10.466 | 0.629 | 0.06227 | 8.095 |
| 7 | 124.921 | 0.007 | 0.236 | 0.101 | 0.255 | 0.051 | 188.451 | 1.803 | 2.911 | 10.476 | 0.629 | 0.06369 | 8.085 |
| 8 | 129.530 | 0.007 | 0.189 | 0.104 | 0.256 | 0.036 | 186.343 | 1.803 | 5.242 | 10.459 | 0.630 | 0.06614 | 8.055 |
| 9 | 138.218 | 0.059 | 0.180 | 0.105 | 0.258 | 0.050 | 190.995 | 1.511 | 5.635 | 17.064 | 0.629 | 0.06620 | 7.855 |
| 10 | 134.863 | 0.007 | 0.249 | 0.115 | 0.269 | 0.014 | 186.842 | 1.794 | 5.704 | 10.341 | 0.629 | 0.06624 | 7.785 |

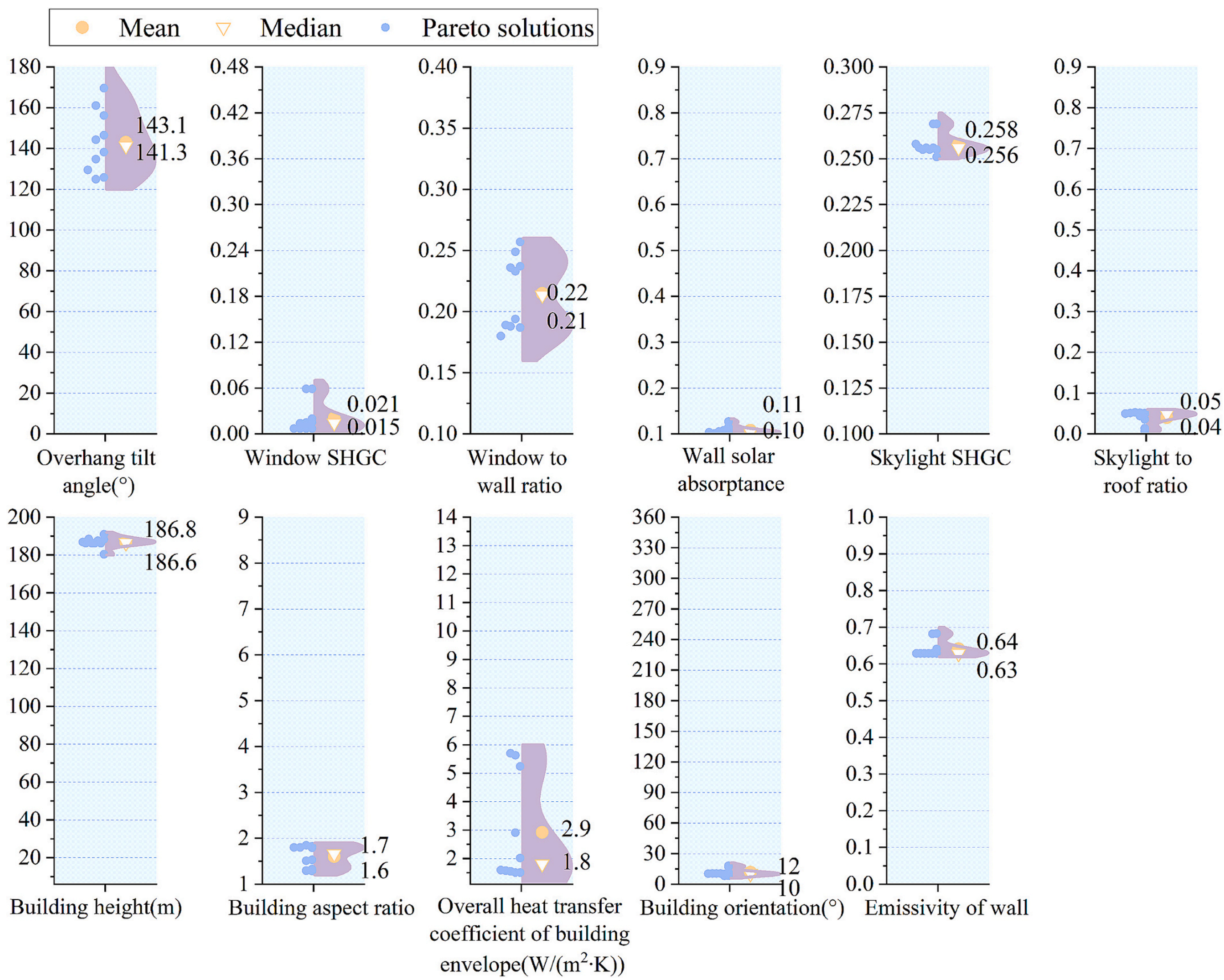


**Fig. 7.** Search range, and mean value, median value and distribution of the Pareto front of the building design variables.

meteorological pattern can lead to a lower air temperature and a higher wind speed in the vertical direction as height increases [68,69], thereby decreasing the cooling loads per unit area [70–73]. It is recommended to consider a lower overall heat transfer coefficient of the building envelope to alleviate both building energy consumption and pedestrian thermal discomfort, which is consistent with the result in previous research [51]. The previous research indicates that the overall heat transfer coefficient of the building envelope is positively correlated with local air temperature changes and negatively correlated with local wind velocity changes. Building with a lower heat transfer coefficient can effectively isolate the external heat, reducing the external surface temperature of the building and leading to lower surrounding air temperature. Additionally, the lower external surface temperature facilitates better airflow around the building, which may enhance the ventilation and mitigate the pedestrian thermal discomfort. Furthermore, the building energy consumption will be reduced by decreasing the amount of external heat entering the indoor environment. An optimal range (i.e., 1.5 to 5.7 W/(m$^2$•K)) is proposed in this test case, and smaller values are not always optimal (i.e., less than 1.5 W/(m$^2$•K)). An extremely low overall heat transfer coefficient of the building envelope may prevent adequate heat dissipation between indoor and outdoor air. As shown in Fig. 5, when the indoor temperature is below the cooling setpoint, this low overall heat transfer coefficient hinders natural ventilation, potentially leading to increased reliance on mechanical ventilation and cooling systems rather than promoting energy-efficient cooling strategies. In the test case, a windward orientation (i.e., 8–18°) helps direct wind flow along the sides of the building, thereby reducing the surrounding air temperature and enhancing both the building energy performance and pedestrian thermal comfort.

### 5.2. Solution evaluation and recommendation based on entropy-TOPSIS method

The entropy-TOPSIS method is utilized for the evaluation of the Pareto optimal solutions to select the best solution maximizing the overall benefits concerning building energy performance and pedestrian thermal comfort. In this study, minimizing the total building energy consumption and mitigating the pedestrian thermal discomfort degree are of equal importance. The scores of the solutions are normalized to the range of 0–1 for ranking. The larger the score obtained by the solution, the better the overall performance of the building design, which will result in a higher ranking for the solution.

The rankings and scores of the ten Pareto optimal solutions evaluated by the entropy-TOPSIS method are shown in Fig. 8. The best solution (Scheme 2) with the highest score (i.e., 0.826) is marked on the Pareto front in Fig. 9. It can be observed that it is the building design scheme that has the total building energy consumption of 0.061kWh/m$^2$ (the second lowest total building energy consumption), 1835.1 kWh for the entire building on a typical summer design day, and the pedestrian thermal discomfort degree of 8.55 °C (the second highest pedestrian thermal discomfort degree) on a typical summer design day. Scheme 2 has a building height of 186 m, building orientation of 12°, building aspect ratio of 1.3, emissivity of wall of 0.7, heat transfer coefficient of building envelope of 1.5 W/(m$^2$•K), overhang tilt angle of 126°, window SHGC of 0.015, window to wall ratio of 0.26, wall solar absorptance of 0.1, skylight SHGC of 0.256, skylight to roof ratio of 0.05. The solution (Scheme 10) with the lowest score (i.e., 0.009) is also marked on the Pareto front in Fig. 9. It can be observed that it has the largest total building energy consumption of 0.066kWh/m2, 1835.1 kWh for the entire building on a typical summer design day, and the lowest pedestrian thermal discomfort degree of 7.785 °C on a typical summer design day. Scheme 10 has a building height of 135 m, building orientation of 10°, building aspect ratio of 1.8, emissivity of wall of 0.629, heat transfer coefficient of building envelope of 5.7 W/(m$^2$•K), overhang tilt angle of 135°, window SHGC of 0.007, window to wall ratio of 0.25, wall solar absorptance of 0.1, skylight SHGC of 0.269, skylight to roof ratio of 0.01.

As the building height is identified as the variable that negatively impacts both total building energy consumption and pedestrian thermal discomfort in previous research, it is considered as a beneficial criterion in this study. That means a larger value can benefit both building energy performance and local microclimate, as proposed in Scheme 2. Meanwhile, as the overall heat transfer coefficient has positive impacts on both total building energy consumption and pedestrian thermal discomfort, it is therefore determined as the cost criterion to be minimized in this study, as proposed in Scheme 2. When compared to historical building design solutions, the recommended best solution (Scheme 2) can save up to 62.9 % (0.103 kWh/m$^2$) of total building energy consumption and 3109.4 kWh for the entire building on a typical summer design day, while mitigating pedestrian thermal discomfort by up to 11.5 % (1.11 K) to prevent unacceptable extreme weather.

### 5.3. Discussion on optimization complexity and computational cost

In this study, the computing time of the design optimization can be reduced by 99.98 % (i.e., from 42,684.44 to 8.89 h) compared with that using conventional simulation methods in the same test condition. In the iterative process of coordinated design optimization for a building and its local microclimate, computing time is primarily spent on numerous simulations of building energy performance and microclimate to evaluate the objectives of various design options. In this study, conventional simulation methods refer to building energy performance simulations using EnergyPlus and CFD microclimate simulations. The computing time required by these conventional methods serves as the baseline for comparison. Each EnergyPlus simulation takes about 4 s, while each CFD simulation takes approximately 5.33 h (19,204 s). In this coordinated optimal design, a total of 8000 evaluations, including 100 populations over 80 generations, are conducted to achieve convergence. Therefore, the total computing time using conventional simulation methods is estimated to be around 42,684.44 h. The proposed surrogate-

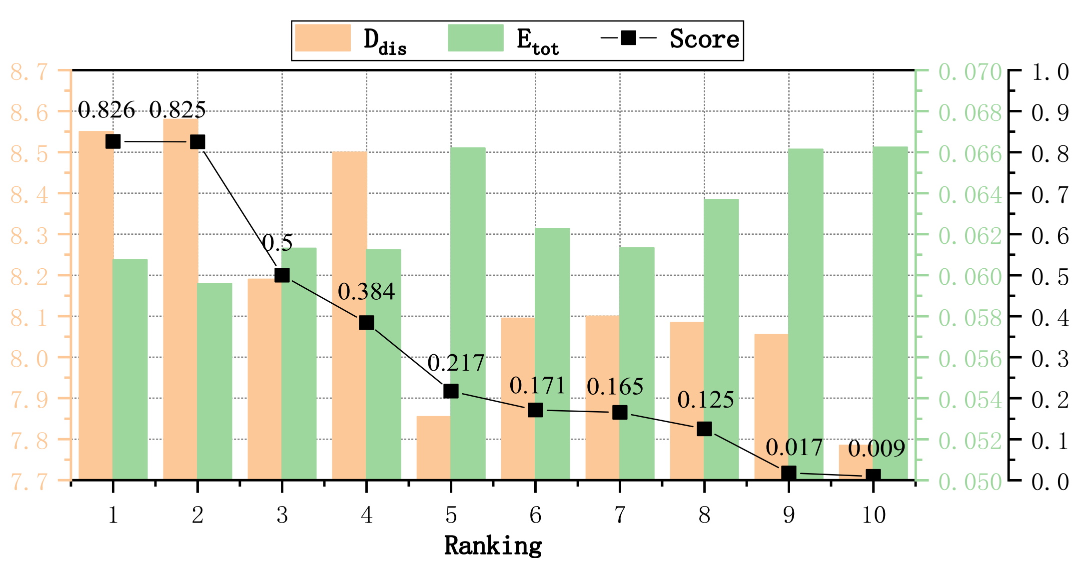


**Fig. 8.** Rankings and scores of the Pareto optimal solutions evaluated by entropy-TOPSIS method.

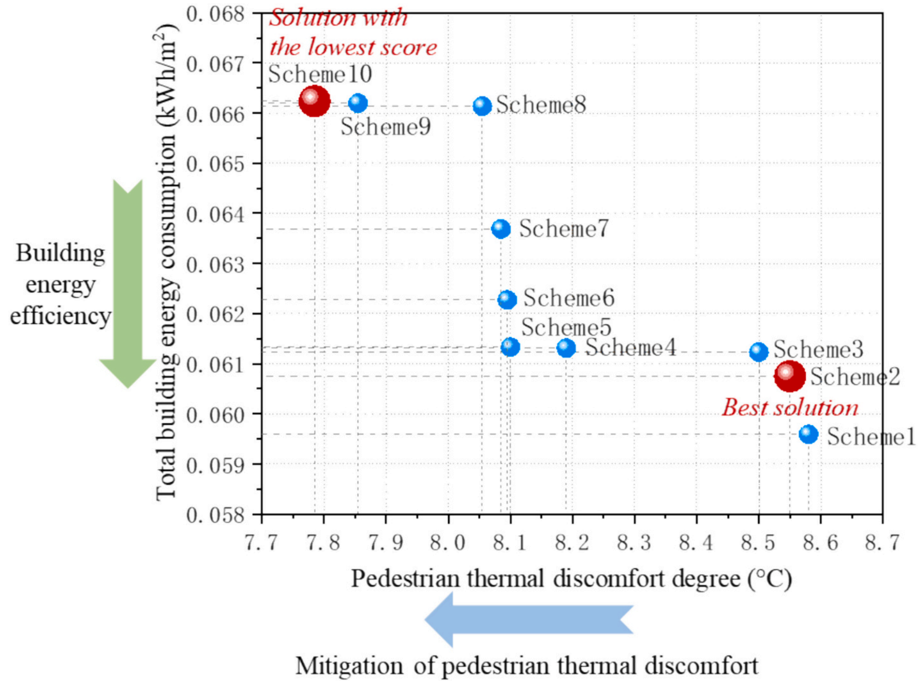


**Fig. 9.** The best solution on the Pareto front.

assisted coordinated design optimization method utilizes automated building performance simulations and local microclimate surrogate models for predicting local microclimate conditions. The computing time for one automated building performance simulation and one local microclimate prediction is approximately 4 s in total. The prediction time for the local microclimate is at the millisecond level for each prediction (excluding the development time costs of the surrogate models). Thus, it takes about 8.89 h for 8000 evaluations to achieve convergence. The device used for computation is a PC with an i7–3770 CPU at 3.40 GHz and Windows 7 Enterprise 64-bit OS. The coordinated design optimization, automated building performance simulation model and local microclimate surrogate model development are conducted in Python 3.2.2 (64-bit).

Even taking into account the time costs for surrogate model development, the proposed method can still save 41,608.75 h and 97.48 % of the total computing time for the coordinated design optimization compared with the conventional simulation methods (i.e., from 42,684.44 to 1075.69 h). The utilization of surrogate models for local microclimate prediction saves a large amount of time compared with the time-consuming CFD simulation. Once the model development is complete, the prediction time is at the millisecond level. To develop the surrogate models, a total of 200 high-resolution CFD simulations are conducted to obtain the training dataset. Each CFD simulation, including the automatic process of mesh improvement, parameter setting, model simulation and result processing, takes about 5.33 h using Fluent 2019 (R3). The total time for developing the SVR-based local air temperature surrogate model (including the time for hyperparameter tuning and data processing) is around 1.65 min, while the time for developing the LightGBM-based local wind velocity surrogate model is around 5.93 min. Thus, the development of the local microclimate surrogate models takes a total of 64,008 min (i.e., 3,840,455 s). In addition, the coordinated design optimization requires about 8.89 h for 8000 evaluations to achieve convergence. Therefore, the total time cost for the coordinated design optimization (including the development time of the surrogate models) amounts to 1075.69 h.

In order to assess the computational cost in the design optimization, a linear model (as shown in Fig. 10) is developed to make to compare the proposed method in this study with the conventional method. In this

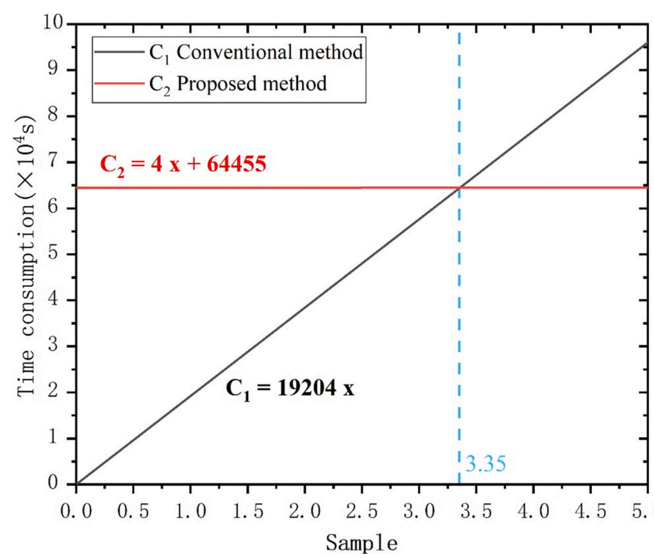


**Fig. 10.** Comparison of computing time for traditional method and proposed method.

model, $x$ is the sampling design solutions (i.e., generations*populations) included in the design optimization. $C_1$ is the computing time for the conventional method. $C_2$ is the computing time including that for surrogate model development. It can be observed in Fig. 10 that when the number of samples exceeds 200, the proposed method offers a significant advantage over the conventional method in terms of computational efficiency. For design optimization involving numerous design variables (i.e., 11 in this study), adequate iterations and samplings are necessary to converge and identify the global optimum solution, and to avoid local optimum. The proposed method provides the designers with a comprehensive and efficient analysis of building design and local microclimate, considering the interaction between them.

## 6. Conclusions

In this study, a coordinated design optimization method is proposed, allowing for the optimization of a building and its microclimate within a practically affordable time frame. It enhances building energy performance while mitigating unacceptable negative impacts on the local microclimate. Based on the results of the optimization case study in subtropical areas, the major conclusions can be summarized as follows.

- The coordinated design optimization of the building and its local microclimate is necessary when certain building design variables lead to conflicting impacts. The Pareto optimal solutions identified by the proposed method can reach compromise building design solutions that balance energy efficiency and pedestrian thermal comfort. These solutions help to reduce total building energy consumption by approximately 59.5–63.6 % (0.097–0.104kWh/m$^2$) while mitigating pedestrian thermal discomfort by about 11.2–19.4 % (1.08–1.88 K) on a typical summer design day in subtropical areas.
- The Pareto front suggests the optimal ranges of building design variables that can minimize building energy consumption while mitigating pedestrian thermal discomfort in the test case in subtropical areas (i.e., window to wall ratio of 0.2–0.3, wall solar absorptance around of 0.1, skylight to roof ratio of 0.01–0.05, building height of 180–191 m, building aspect ratio of 1.3–1.8, overall heat transfer coefficient of building envelope of 1.5–5.7 W/(m$^2$•K), and building orientation of 8–18°).
- The best design solution recommended by the entropy-TOPSIS method, which features a larger building height and a smaller overall heat transfer coefficient within the optimal range, can save up to 62.9 % (0.103 kWh/m$^2$) of total building energy consumption and 3109.4 kWh for the entire building on a typical summer design day, while mitigating pedestrian thermal discomfort by up to 11.5 % (1.11 K) to prevent unacceptable extreme weather in subtropical areas.
- The surrogate-assisted coordinated design optimization method proposed in this study can reduce the computation time by 99.98 % (i.e., from 42,684.44 to 8.89 h), and reduce the total computational cost by 97.48 % (i.e., from 42,684.44 to 1075.69 h) compared with conventional simulation methods. When the samples exceed 200, the proposed method has a significant advantage over the traditional method in terms of time savings.

In this study, only the most unfavorable weather condition is used to evaluate the performance of coordinated optimal design. This approach assesses representative pedestrian thermal discomfort and total building energy consumption under extreme climate conditions while significantly reducing computing costs. Performances under other conditions are not considered, and annual total building energy consumption is not addressed. The optimization results are validated with a test case in subtropical regions, and recommendations are provided for these areas.

Theoretically, the coordinated design optimization method can address the optimization of individual buildings and their local microclimates across different climate zones and building types due to the applicability of building design variables, optimization objectives, automated building performance simulation models, and local microclimate surrogate models in various climate zones and building types. In future work, it will be applied to building cases of different types in different climate zones for validation and comparison. More constraints (i.e., construction requirements, and economic factors) will be take in into consideration from a practical application perspective. Optimization objectives related to energy system performance in the HVAC system design stage will be considered. The energy performance model will be validated based on actual equipment and systems. The energy model will be validated based on actual equipment and systems. More changes in the weather conditions will be incorporated. This method will be applied to groups of buildings or entire districts, considering the real interactions between buildings and other entities, such as trees and shading systems, to enhance its application potential and value.

## CRediT authorship contribution statement

**Zeming Zhao:** Writing – original draft, Validation, Software, Methodology, Investigation, Formal analysis, Data curation, Conceptualization. **Hangxin Li:** Writing – review & editing, Supervision, Project administration, Methodology, Funding acquisition, Conceptualization. **Shengwei Wang:** Writing – review & editing, Supervision, Project administration, Funding acquisition.

## Declaration of competing interest

The authors declare that they have no known competing financial interests or personal relationships that could have appeared to influence the work reported in this paper.

## Acknowledgment

The research work presented in this paper is funded by Shenzhen Science and Technology Innovation Commission (Grant number: KCXST20221021111203007) and General Research Grant (15221623) of the Research Grant Council (RGC) of the Hong Kong SAR.

## Data availability

Data will be made available on request.

## References

[1] International energy agency. Key World Energy Statistics; 2017.
[2] Energy and climate in the urban built environment[M]. Routledge; 2013.
[3] Mosteiro-Romero M, Maiullari D, Pijpers-van Esch M, Schlueter A. An integrated microclimate-energy demand simulation method for the assessment of urban districts. Front Built Env 2020;6:553946.
[4] Shen P, Liu J, Wang M. Fast generation of microclimate weather data for building simulation under heat island using map capturing and clustering technique. Sustain Cities Soc 2021;71:102954.
[5] Palme M, Inostroza L, Villacreses G, Lobato-Cordero A, Carrasco C. From urban climate to energy consumption. Enhancing building performance simulation by including the urban heat island effect. Energ Buildings 2017;145:107–20.
[6] Cui Y, Yan D, Hong T, Ma J. Temporal and spatial characteristics of the urban heat island in Beijing and the impact on building design and energy performance. Energy 2017;130:286–97.
[7] Merlier L, Frayssinet L, Johannes K, Kuznik F. On the impact of local microclimate on building performance simulation. Part II: Effect of external conditions on the dynamic thermal behavior of buildings. In: Building simulation. vol. 12. Tsinghua University Press; 2019, October. p. 747–57.
[8] Allegrini J, Carmeliet J. Coupled CFD and building energy simulations for studying the impacts of building height topology and buoyancy on local urban microclimates. Urban Clim 2017;21:278–305.
[9] Merlier L, Frayssinet L, Johannes K, Kuznik F. Graa. Part I: Prediction of building external conditions. In: Building simulation. vol. 12. Tsinghua University Press; 2019 October. p. 735–46.
[10] Dimoudi A, Kantzioura A, Zoras S, Pallas C, Kosmopoulos P. Investigation of urban microclimate parameters in an urban center. Energ Buildings 2013;64:1–9.
[11] Ignatius M, Wong NH, Jusuf SK. Urban microclimate analysis with consideration of local ambient temperature, external heat gain, urban ventilation, and outdoor thermal comfort in the tropics. Sustain Cities Soc 2015;19:121–35.
[12] Zinzi M, Carnielo E, Mattoni B. On the relation between urban climate and energy performance of buildings. A three-years experience in Rome, Italy. Appl Energy 2018;221:148–60.
[13] Xie X, Sahin O, Luo Z, et al. Impact of neighbourhood-scale climate characteristics on building heating demand and night ventilation cooling potential[J]. Renew Energy 2020;150:943–56.
[14] Li H, Wang S. Coordinated optimal design of zero/low energy buildings and their energy systems based on multi-stage design optimization. Energy 2019;189.
[15] Li H, Wang S, Yan J. Coordinated robust optimal design of building envelope and energy systems for zero/low energy buildings considering uncertainties. Appl Energy 2020;265.
[16] Li Q, Zhang L, Zhang L, Wu X. Optimizing energy efficiency and thermal comfort in building green retrofit. Energy 2021;237:121509.
[17] Wang Y, Wei C. Design optimization of office building envelope based on quantum genetic algorithm for energy conservation - sciencedirect. J Build Eng 2021;35:102048.

[18] Bamdad K, Cholette ME, Omrani S, Bell J. Future energy-optimised buildings — addressing the impact of climate change on buildings. Energ Build 2020;231(2):110610.
[19] Kiss B, Szalay Z. Modular approach to multi-objective environmental optimization of buildings. Autom Constr 2020;111:103044.
[20] Giouri ED, Tenpierik M, Turrin M. Zero energy potential of a high-rise office building in a mediterranean climate: using multi-objective optimization to understand the impact of design decisions towards zero-energy high-rise buildings. Energy Build 2020;(Feb):209.
[21] Bui DK, Nguyen TN, Ghazlan A, Ngo NT, Ngo TD. Enhancing building energy efficiency by adaptive façade: a computational optimization approach. Appl Energy 2020;265:114797.
[22] Malik R, Dua S, Shoran P, Nain A. Enhancing security and resource optimization in iot applications with blockchain inclusion. In: 2nd international conference on futuristic technologies (INCOFT). IEEE; 2023.
[23] Sun Z, Cao Y, Wang X, Yu J. Multi-objective optimization design for windows and shading configuration: considering energy consumption, thermal environment, visual performance and sound insulation effect. Int J Energy Environ Eng 2021;12(4):805–36.
[24] Chen KW, Janssen P, Schlueter A. Multi-objective optimisation of building form, envelope and cooling system for improved building energy performance. Autom Constr 2018;94:449–57.
[25] Jiang M, Araji MT. Multivariate optimization towards energy balance with geometric constraints of building design and urban space intensity. Sustain Energy Technol Assess 2023;57:103124.
[26] Feng J, Luo X, Gao M, Abbas A, Xu YP, Pouramini S. Minimization of energy consumption by building shape optimization using an improved Manta-ray foraging optimization algorithm. Energy Rep 2021;7:1068–78.
[27] Rabani M, Madessa HB, Nord N. Achieving zero-energy building performance with thermal and visual comfort enhancement through optimization of fenestration, envelope, shading device, and energy supply system. Sustain Energy Technol Assess 2021;44:101020.
[28] Ilbeigi M, Ghomeishi M, Dehghanbanadaki A. Prediction and optimization of energy consumption in an office building using artificial neural network and a genetic algorithm. Sustain Cities Soc 2020;61:102325.
[29] Zhu L, Wang B, Sun Y. Multi-objective optimization for energy consumption, daylighting and thermal comfort performance of rural tourism buildings in North China. Build Environ 2020;176:106841.
[30] Jalali Z, Noorzai E, Heidari S. Design and optimization of form and facade of an office building using the genetic algorithm. Sci Technol Built Environ 2020;26(2):128–40.
[31] Wu Y, Zhan Q, Quan SJ, Fan Y, Yang Y. A surrogate-assisted optimization framework for microclimate-sensitive urban design practice. Build Environ 2021;195(1–3):107661.
[32] Wu Y, Zhan Q, Quan SJ. Improving local pedestrian-level wind environment based on probabilistic assessment using gaussian process regression. Build Environ 2021;205:108172.
[33] Huang C, Zhang G, Yao J, Wang X, Calautit JK, Zhao C, et al. Accelerated environmental performance-driven urban design with generative adversarial network. Build Environ 2022;224:109575.
[34] Weerasuriya A, Zhang X, Bin L, Tse KT, Liu CH. Optimizing lift-up design to maximize pedestrian wind and thermal comfort in 'hot-calm' and 'cold-windy' climates. Sustain Cities Soc 2020;58:102146.
[35] Tanaka H, Matsuoka Y, Kawakami T, Azegami Y, Yamamoto M, Ohtake K, et al. Optimization calculations and machine learning aimed at reduction of wind forces acting on tall buildings and mitigation of wind environment. Int J High-Rise Build 2019;8(4):291–302.
[36] Düring Serjoscha, Chronis A, Koenig R. Optimizing Urban Systems: integrated optimization of spatial configurations. Symposium Simulation Architecture Urban Design 2020:1–7.
[37] Kaseb Z, Hafezi M, Tahbaz M, Delfani S. A framework for pedestrian-level wind conditions improvement in urban areas: CFD simulation and optimization. Build Environ 2020;184:107191.
[38] Zhang J, Cui P, Song H. Impact of urban morphology on outdoor air temperature and microclimate optimization strategy base on pareto optimality in Northeast China. Build Environ 2020;180(1101):107035.
[39] Du Y, Mak CM, Li Y. A multi-stage optimization of pedestrian level wind environment and thermal comfort with lift-up design in ideal urban canyons. Sustain Cities Soc 2019;46.
[40] Wang SS, Yi YK, Liu NX. Multi-objective optimization (moo) for high-rise residential buildings' layout centered on daylight, visual, and outdoor thermal metrics in China. Build Environ 2021;108263(224).
[41] Allen-Dumas MR, Sweet LT, Brelsford C. Determining optimal resolution for urban terrain inputs to microclimate modeling. Authorea Preprints; 2022.
[42] Deb K, Pratap A, Agarwal S, Meyarivan T. A fast and elitist multiobjective genetic algorithm: nsga-ii. IEEE Trans Evol Comput 2002;6(2):182–97.
[43] Zhao Z, Li H, Wang S. Identification of the key design parameters of zero/low energy buildings and the impacts of climate and building morphology. Appl Energy 2022;328:120185.
[44] Mosteiro-Romero M, Maiullari D, Pijpers-van Esch M, Schlueter A. An integrated microclimate-energy demand simulation method for the assessment of urban districts. Front Built Env 2020;6:553946.
[45] Liu J, Heidarinejad M, Nikkho SK, Mattise NW, Srebric J. Quantifying impacts of urban microclimate on a building energy consumption—a case study. Sustainability 2019;11(18):4921.
[46] Tsoka S. Investigating the relationship between urban spaces morphology and local microclimate: a study for Thessaloniki. Procedia Environ Sci 2017;38:674–81.
[47] Allegrini J, Dorer V, Carmeliet J. Influence of morphologies on the microclimate in urban neighbourhoods. J Wind Eng Ind Aerodyn 2015;144:108–17.
[48] Middel A, Häb K, Brazel AJ, Martin CA, Guhathakurta S. Impact of urban form and design on mid-afternoon microclimate in Phoenix local climate zones. Landsc Urban Plan 2014;122:16–28.
[49] Zhao Z, Li H, Wang S. Machine learning-based surrogate models for fast impact assessment of a new building on urban local microclimate at design stage. Build Environ 2024;112142.
[50] Ng E, Cheng V. Urban human thermal comfort in hot and humid Hong Kong. Energ Buildings 2012;55:51–65.
[51] Zhao Z, Li H, Wang S. The mutual impacts of individual building design and local microclimate in high-density cities and the major influential parameters. In: Building simulation. Tsinghua University Press; 2024, December. p. 1–23.
[52] Design standard for energy efficiency of residential buildings in hot summer and warm winter zone, 2012 JGJ 75–2012.
[53] Design standard for energy efficiency of public buildings, 2015 GB 50189–2015.
[54] Technical standard for near zero energy buildings, 2019 GB/T 51350–2019.
[55] Inanici MN, Demirbilek FN. Thermal performance optimization of building aspect ratio and south window size in five cities having different climatic characteristics of Turkey. Build Environ 2000;35(1):41–52.
[56] Huang W, Shuai B, Sun Y, Wang Y, Antwi E. Using entropy-TOPSIS method to evaluate urban rail transit system operation performance: the China case. Transp Res Part A: Policy Pract 2018;111:292–303.
[57] Huang J. Combining entropy weight and TOPSIS method for information system selection. In: In 2008 ieee conference on cybernetics and intelligent systems. IEEE; 2008, September. p. 1281–4.
[58] Ding C, Lam KP. Data-driven model for cross ventilation potential in high-density cities based on coupled CFD simulation and machine learning. Build Environ 2019;165:106394.
[59] Calzolari G, Liu W. Deep learning to replace, improve, or aid CFD analysis in built environment applications: a review. Build Environ 2021;206:108315.
[60] Tominaga Y, Mochida A, Shirasawa T, Yoshie R, Kataoka H, Harimoto K, et al. Cross comparisons of CFD results of wind environment at pedestrian level around a high-rise building and within a building complex. J Asian Architecture Build Eng 2004;3(1):63–70.
[61] Helton JC, Davis FJ. Latin hypercube sampling and the propagation of uncertainty in analyses of complex systems. Reliab Eng Syst Saf 2003;81(1):23e69.
[62] Chen X, Yu L, Liu LY, Yang L, Xu S, Wu J. Multi-objective shape optimization of autonomous underwater vehicle by coupling CFD simulation with genetic algorithm. Ocean Eng 2023;286:115722.
[63] Afzal A, Kim KY, Seo JW. Effects of Latin hypercube sampling on surrogate modeling and optimization. Int J Fluid Machinery Syst 2017;10(3):240–53.
[64] Pianosi F, Beven K, Freer J, Hall JW, Rougier J, Stephenson DB, et al. Sensitivity analysis of environmental models: a systematic review with practical workflow. Environ Model Softw 2016;79:214–32.
[65] Pang Z, O'Neill Z, Li Y, Niu F. The role of sensitivity analysis in the building performance analysis: a critical review. Energ Buildings 2020;209:109659.
[66] Mostafavi F, Tahsildoost M, Zomorodian Z. Energy efficiency and carbon emission in high-rise buildings: a review (2005-2020). Build Environ 2021;206:108329.
[67] Wang Y, Mauree D, Sun Q, Lin H, Scartezzini JL, Wennersten R. A review of approaches to low-carbon transition of high-rise residential buildings in China. Renew Sust Energ Rev 2020;131:109990.
[68] Ge J, Wang Y, Zhou D, Gu Z, Meng X. Building energy demand of urban blocks in Xi'an, China: impacts of high-rises and vertical meteorological pattern. Build Environ 2023;244:110749.
[69] Tang Y, Sun T, Luo Z, Omidvar H, Theeuwes N, Xie X, et al. Urban meteorological forcing data for building energy simulations. Build Environ 2021;204:108088.
[70] Yu H, Wang M, Lin X, Guo H, Liu H, Zhao Y, et al. Prioritizing urban planning factors on community energy performance based on GIS-informed building energy modeling. Energ Build 2021;249:111191.
[71] Liu K, Xu X, Zhang R, Kong L, Wang W, Deng W. Impact of urban form on building energy consumption and solar energy potential: a case study of residential blocks in Jianhu, China. Energy Build 2023;280:112727.
[72] Yoon YB, Seo B, Koh BB, Cho S. Performance analysis of a double-skin façade system installed at different floor levels of high-rise apartment building. J Build Eng 2019;26:100900.
[73] Du J, Pan W. Cooling-related energy uses and adaptive behaviors in high-rise residential buildings in the subtropical climate: a case study in Hong Kong. Build Environ 2022;223:109456.